Numerical Computation of Fat Layer Effects on Microwave Near-Field Radiation to the Abdomen of a Full-Scale Human Body Model

H.-R. Chuang

Abstract— **Numerical computation results of fat layer effects on the microwave near field radiation to the abdomen of a three-dimensional (3-D) full-scale human body model are presented. The human body is modeled as a 3-D homogeneous muscle phantom with a fat layer covering the abdomen part. The dipole wire-antenna located proximate to the abdomen is used as the microwave radiation source at 915 MHz. This is to study the effects on hyperthermia heating by using the microwave applicator (at 915 MHz) or the near-field exposure from the proximate handset antenna to the human body at ISM band wireless communication band (902–928 MHz). Coupled integral equations (CIE) and the method of moments (MoM) are employed to numerically compute electromagnetic (EM) energy deposition specific absorption rate (SAR) from the radio frequency (RF) antenna applicator into the proximate fat layer covered abdomen. The antenna input impedance (proximate to the body), return loss (RL), and the resonant antenna length (proximate to the body) will also be numerically determined to increase the microwave power delivered into the body. The study of fat layer effects is important for microwave hyperthermia applications. It is also important for the investigation of the potential health hazard from the near-field radiation of a wireless communication antenna.**

I. Introduction

In RESEARCH on microwave hyperthermia heating to treat tumors inside the human body, the effect of the fat overlaying the muscle tissue, especially the abdomen covered with a fat layer, is a significant issue that requires investigation [1], [2]. Since the conductivity and permittivity of the fat tissue are much smaller than those of muscle tissue, the fat layer will behave like a "shielding" structure and cause microwave power to not be able to effectively penetrate into the muscle tissue to heat the tumors. Moreover, the energy distribution may accumulate in the fat layer and cause heating damage to the fat tissue. Previously reported measurements [1] show the complex heating patterns in the tissue due to different fat thickness. Since the near-field exposure of the microwave applicator is very complicated in an inhomogeneous, bilayered medium, it is very important to study the fat layer effect on microwave hyperthermia heating for effectiveness and safety in clinical applications. On the other hand, for the rapidly growing wireless communication industries, concern exists for the potential health hazard due to radiation of the wireless communication antenna. When the radio telephone is in the pocket, the antenna can be near to the abdomen. In this case, special concern for pregnant women exists for the dose of EM energy from the nearby radiating antenna into the abdomen and the unborn baby. The effect of the fat layer overlaying the muscle tissue of the abdomen is important for this EM dose assessment.

Much research on the EM interaction of the microwave antenna with the human body has focused on the head. The popular EM computational method, the finite-difference time-domain (FDTD) method [3], [4] used in this research problem usually includes only the head in the computation [5]–[7] because of the usual operating position of the radio telephone. Moreover, with the FDTD method the computation of the interaction between the antenna and a three-dimensional (3-D) full-scale human body will take enormous computer memory and CPU time. Recently, a 3-D computer simulation in deep regional hyperthermia used the FDTD method to compute the specific absorption rate (SAR) distribution of the body [8]. In [8], only a section of the body has been modeled and included in computation, and the radio frequency (RF) dipole applicator is operated below 100 MHz. To compute the SAR distribution at much higher frequencies (for example, 915 MHz), the cell dimension of the body and dipole applicator may become too small generating an enormous number of modeling cells for the whole body computation. For this paper we use the coupled integral equations (CIE) and the method of moments (MoM) to conduct the numerical computation. EM interaction of a full-scale body model can be performed more efficiently with the convenient nonuniform cells modeling.

In this research a thin-wire dipole is used as the microwave hyperthermia RF applicator or the wireless communication antenna. Since the interest is to investigate the fat layer effects, a full-scale human phantom of homogeneous muscle tissue with a fat-layer covering the abdomen part with various thickness is used for computer numerical simulation. The penetrating energy from the radiating antenna into the proximate fat-layer-covered abdomen will be numerically computed at 915 MHz. The dipole antenna input impedance and the return loss (RL) can be computed. Optimized antenna length will also be numerically determined to let the hyperthermia RF antenna applicator effectively deliver the microwave power into the body tissue. SAR distribution profiles are computed and plotted.

Manuscript received March 25, 1996; revised September 23, 1996. This work was supported by the National Science Council of the Republic of China under Grant NSC 82-0420-E006-467.

The author is with the Department of Electrical Engineering, National Cheng Kung University, Tainan, Taiwan, R.O.C. (e-mail: chuangh@eembox.ncku.edu.tw).

Publisher Item Identifier S 0018-9480(97)00282-2.

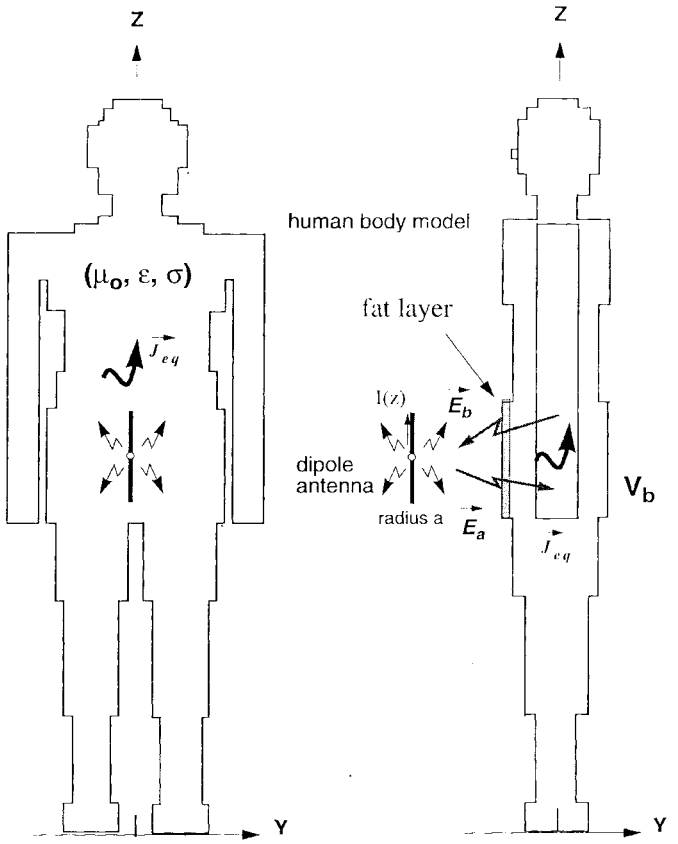

Fig. 1. Illustration of the EM interaction of a dipole wire antenna with a human body model.

II. Computation Modeling

A. CIE Formulation

The method of coupled integral equations (CIE) is used to formulate EM coupling between a dipole thin-wire antenna and a human body model [9], [10]. The coupled integral equations consist of the electric field integral equation (EFIE) for the induced electric field inside the body and the Hallen's-type integral equation (HIE) for the antenna current distribution with mutual coupling terms. The MoM is then used for numerical solution. The following physical quantities of the EM interaction mechanism are to be calculated:

1) the current distribution and the input impedance (and hence the input return loss) of the dipole antenna proximate to the human body;
2) the induced EM fields and the deposited EM energy distribution (SAR) in the body from the nearby radiating dipole antenna;
3) the input power of the dipole antenna, the radiation power to free space, and the power absorbed by the body. The above quantities can be used to check the computation accuracy since the antenna input power should be equal to the sum of the radiation power (to free space) and the body-absorbed power.

Consider the situation of a human body close to a nearby radiating thin-wire antenna, as shown in Fig. 1. The electric

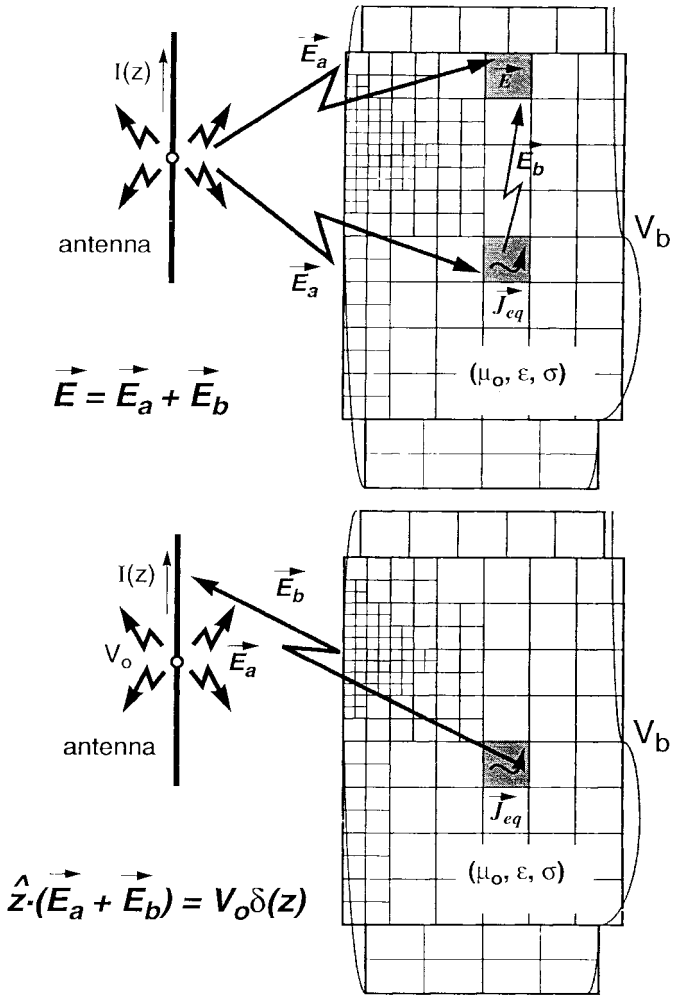

Fig. 2. Illustration of EM interaction mechanism between a dipole antenna and a human body and nonuniform cubic cells modeling for the body model.

parameters of the human body are expressed as

$$\text{conductivity: } \sigma = \sigma(\omega, \vec{r}); \quad \text{permittivity: } \epsilon = \epsilon(\omega, \vec{r})$$
$$\text{permeability: } \mu = \mu_0$$

where the body is assumed to be a nonmagnetic medium. The incident EM field $(\vec{E}^a, \vec{H}^a)$ maintained by the antenna will generate induced conduction and polarization currents $\vec{J}_{\text{eq}}$ inside the body, and these induced currents produce a scattered EM field $(\vec{E}^b, \vec{H}^b)$. The total EM field $(\vec{E}, \vec{H})$ is the sum of the incident field and the scattered field. Also the boundary condition for the tangential electric field at points along the surface of the perfectly conducting antenna excited by a delta-gap generator leads to

$$\hat{s}\cdot\{\vec{E}^a(s) + \vec{E}^b(s)\} = -V_0\delta(s) \tag{1}$$

where V_0 is the driving-point input voltage, s is a field point on the antenna surface, and $\hat{s}$ is a unit vector at s tangential to the antenna surface. Fig. 2 depicts the illustration of this EM interaction mechanism.

The solutions for the antenna current distribution $I_a(z)$ of a z-oriented linear dipole antenna (with half-length h and radius a) and the total induced electric field $\vec{E}(\vec{r})$ inside the body, as

shown in Fig. 1, can be written as a pair of coupled integral equations by the dyadic Green's function techniques:

$$\left\{1+\frac{\tau(\vec{r})}{3j\omega\epsilon_0}\right\}\vec{E}(\vec{r})-PV\int_{V_b}\tau(\vec{r}')(\vec{E}(\vec{r}')\cdot\bar{G}(\vec{r},\vec{r}'))dv' = \int_{-h}^{h} I_a(z')(\hat{z}\cdot\bar{G}(\vec{r},z'))dz' \tag{2}$$

$$\int_{-h}^{h} I_a(z')K_a(z,z')dz' + A\cos k_0 z + B\sin k_0 z + j\frac{4\pi}{\eta_0}\int_0^z E_z^b(u)\sin k_0(z-u)du = -j\frac{2\pi}{\eta_0}V_0\sin k_0|z| \tag{3}$$

where the symbol *PV* denotes the principal value of the integral carried out by excluding an infinitesimally small volume surrounding the field point and A and B are two unknown constants. $E_z^b(z)$ is the z component of the scattered electric field from the body at the antenna surface

$$E_z^b(z)=PV\int_{V_b}\tau(\vec{r}')(\vec{E}(\vec{r}')\cdot\bar{G}(z,\vec{r}'))dv' \tag{4}$$

$$\bar{G}(\vec{r},\vec{r}')=-j\omega\mu_0\left[\bar{I}+\frac{\nabla\nabla}{k_0^2}\right]G_0(\vec{r},\vec{r}');$$

$$G_0(\vec{r},\vec{r}')=\frac{e^{-jk_0|\vec{r}-\vec{r}'|}}{4\pi\mid\vec{r}-\vec{r}'\mid}$$

$$\tau(\vec{r})=\sigma(\vec{r})+j\omega(\epsilon(\vec{r})-\epsilon_0);\ k_0=\omega\sqrt{\mu_0\epsilon_0};\eta_0=\sqrt{\mu_0/\epsilon_0}$$

$$K_a(z,z')=\exp(-jk_0R)/R;\ R=\sqrt{(z-z')^2+a^2}.$$

$\vec{r}$ (or $\vec{r}'$) is a field (or source) point inside V_b, z (or z') is a field (or source) point along the antenna surface, and $\tau(\vec{r})$ is the complex conductivity that defines the induced conduction and polarization current density $\vec{J}_{\rm eq}(\vec{r})$ inside the body

$$\vec{J}_{\rm eq}(\vec{r})=\tau(\vec{r})\vec{E}(\vec{r});\ \tau(\vec{r})=\sigma(\vec{r})+j\omega(\epsilon(\vec{r})-\epsilon_0). \tag{5}$$

Equation (2) is the EFIE and (3) is the HIE, with mutual coupling terms appearing in both equations.

B. Method of Moments Solution

Equations (2) and (3) are solved numerically by MoM. The antenna is partitioned into N_a segments and the body is subdivided into N_b nonuniform cubic cells. Pulse function expansions are used to approximate the unknown E-fields ($\vec{E}_b(\vec{r})$) in the body and antenna currents $I_a(z)$. Delta function testing is employed to point match in each subvolume of the body and at each partition of the antenna. This leads to a system of $(N_a+3N_b)\times(N_a+3N_b)$ complex/dense matrix equation:

$$\begin{bmatrix} (G_{aa}) & (G_{ab}^x) & (G_{ab}^y) & (G_{ab}^z) \\ (G_{ba}^x) & (G_{bb}^{xx}) & (G_{bb}^{xy}) & (G_{bb}^{xz}) \\ (G_{ba}^y) & (G_{bb}^{yx}) & (G_{bb}^{yy}) & (G_{bb}^{yz}) \\ (G_{ba}^z) & (G_{bb}^{zx}) & (G_{bb}^{zy}) & (G_{bb}^{zz}) \end{bmatrix}\begin{bmatrix} (I_a) \\ (E_b^x) \\ (E_b^y) \\ (E_b^z) \end{bmatrix} = \begin{bmatrix} ((-j2\pi V_0/\eta_0)\sin k_0|z|) \\ (0) \\ (0) \\ (0) \end{bmatrix} \tag{6}$$

where (G_{aa}) is a $(N_a\times N_a)$ submatrix, (G_{ab}) is $(N_a\times N_b)$, (G_{ba}) is $(N_b\times N_a)$, (G_{bb}) is $(N_b\times N_b)$, and all others are corresponding column vectors. In the computation of the matrix elements, each cubic cell is again subdivided into n_v^3 subcells for numerical integration. In the sense, this is like having $n_v^3\times N_b$ cubic cells. This scheme can increase the MoM computation accuracy without enlarging the matrix equation order. The cost is approximately nv^3 times CPU time. The antenna current and the induced electric field inside the body can be determined by solving the matrix equation above. The antenna input impedance Z_i, the input return loss (RL), and input power P_i are then calculated

$$Z_i=V_0/I_0;\quad P_i=V_0I_0^*/2 \tag{7}$$

where I_0 is the antenna input-terminal current.

C. EM Energy Deposition: Body-Absorbed Power and SAR

Once the induced electric field inside the body is known, the SAR in the nth cell of the body and the total power absorbed by the body P_b can then be determined

$$\mathrm{SAR}(n)=\left[\sigma_n\left(E_b^x(n)\right)^2+\sigma_n\left(E_b^y(n)\right)^2+\sigma_n\left(E_b^z(n)\right)^2\right]/2 \tag{8}$$

$$P_b=\sum_{n=1}^{N_b}\mathrm{SAR}(n)(\Delta V_nG_n) \tag{9}$$

where ΔV_n is the volume of nth cell and σ_n and G_n are the conductivity and the mass density of the tissue in the nth cell.

D. Radiation Power to Free Space from Antenna and Body

The total radiation field that is contributed by the antenna radiating field (to free space) and the body scattering field can also be determined now. The total radiation field $\vec{E}^r(\vec{r})$ at a far-zone point consists of two parts, the antenna radiated field $\vec{E}_a^r(\vec{r})$ and the body scattering field $\vec{E}_b^r(\vec{r})$

$$\vec{E}^r(\vec{r})=\vec{E}_a^r(\vec{r})+\vec{E}_b^r(\vec{r}). \tag{10}$$

The body scattering field can be expressed as the radiation field of the induced current in the body. Based on the Stratton and Chu's formula [11], $\vec{E}_a^r(\vec{r})$ and $\vec{E}_b^r(\vec{r})$ can be written as

$$\vec{E}_a^r(\vec{r})=-j\eta_0k_0\frac{e^{-jk_0r}}{4\pi r}\int_{-h}^{h}\hat{\theta}[-I_a(z')\sin\theta]\times e^{jk_0(z'\cos\theta)}dz' \tag{11}$$

$$\vec{E}_b^r(\vec{r})=-j\eta_0k_0\frac{e^{-jk_0r}}{4\pi r}\times\int_{V_b}\{\hat{\theta}[J_{\rm eq}^x(\vec{r}')\cos\theta\cos\phi+J_{\rm eq}^y(\vec{r}')\times\cos\theta\sin\phi-J_{\rm eq}^z(\vec{r}')\sin\theta] +\hat{\phi}[-J_{\rm eq}^x(\vec{r}')\sin\phi+J_{\rm eq}^y(\vec{r}')\cos\phi]\}\times e^{jk_0(x'\sin\theta\cos\phi+y'\sin\theta\sin\phi+z'\cos\theta)}dv' \tag{12}$$

where I_a is the dipole antenna current and $J_{\rm eq}^x$, $J_{\rm eq}^y$, and $J_{\rm eq}^z$ are the x, y, and z component of the equivalent current

TABLE I
COMPUTATIONAL RESULTS OF THE SAR's, THE BODY-ABSORBED POWER, AND THE RADIATION POWER OF A 915-MHz DIPOLE ANTENNA APPLICATOR IN FRONT OF THE ABDOMEN OF A HUMAN BODY MODEL WITHOUT A FAT LAYER

		in front of abdomen: without a fat layer					
Antenna Location (cm)	∞ (in free space)	2.5	2.0	1.5	1.0	0.5	0.5
915 MHz dipole antenna half-length (cm)	7.7	7.7	7.7	7.7	7.7	7.7	7.4
(radius = 0.127 cm)							
input impedance (Ω)	75	44+j5.4	42+j1.3	43-j2.4	49-j2.4	69+j12	65-j6.0
input return loss (RL) to 50 Ω (dB)		21	21	22	32	14.5	17
input power P_i (W)*	1	1	1	1	1	1	1
radiation power (to free space) P_{rad} (W)	1	0.435	0.327	0.215	0.120	0.055	0.030
body-absorbed power P_b (W)	—	0.571	0.674	0.776	0.879	0.973	0.989
sum of P_{rad} & P_b (W)	—	1.006	1.001	0.991	0.999	1.028	1.019
computation error (%)	—	0.6	0.1	0.9	0.1	2.8	1.9
peak-SAR (mW/g)	—	4.70	6.83	9.87	14.20	20.04	20.8
average-SAR (mW/g)	—	0.009	0.01	0.013	0.015	0.016	0.017

* The antenna input power is kept to be 1 W for comparison.

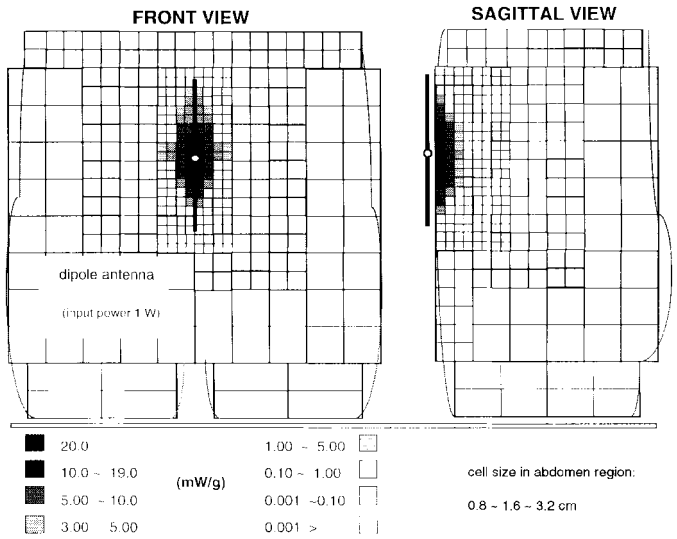

Fig. 3. 915-MHz SAR profile in the abdomen region (without a fat layer) of a human body model. The dipole antenna applicator (h = 7.7 cm) is in front of the abdomen with a distance of 0.5 cm and the antenna input power in 1 W.

density induced inside the body [as shown in (5)]. $\hat{\theta}$ and $\hat{\phi}$ are the elevation and azimuth angle unit vectors in spherical coordinates for far-field representation.

The above integrals can computed numerically from the determined numerical value of the antenna and induced body currents. The radiation power to free space from the coupled system of the antenna and the body is then determined by integrating the radiation power density over a far-zone spherical surface

$$P_{\text{rad}} = \oint_s \frac{1}{2}(\vec{E}^r \times \vec{H}^{r*}) \cdot d\vec{s} = \frac{1}{2\eta_0}\int_0^{2\pi}\int_0^{\pi} |\vec{E}^r|^2 r^2 \sin\theta d\theta d\phi \qquad (13)$$

where $\vec{E}^r$ is in (10). The radiation power (P_{rad}) and the body absorbed power P_b can also be used to compare with the antenna input power P_i to check the EM coupling computation accuracy, since P_i should be equal to the sum of P_{rad} and P_b.

$$\text{computation error} = \frac{|P_i - (P_{\text{rad}} + P_b)|}{P_i}. \qquad (14)$$

III. NUMERICAL RESULTS

As shown in Fig. 1, a realistically shaped 3-D human body model with a height of 178 cm was constructed for numerical study. The dipole antenna is located adjacent to the abdomen. The human body is modeled as a homogeneous

TABLE II
COMPUTATIONAL RESULTS OF THE SAR's, THE BODY-ABSORBED POWER, AND THE RADIATION POWER OF A 915-MHz DIPOLE ANTENNA APPLICATOR IN FRONT OF THE ABDOMEN OF A HUMAN BODY MODEL WITH AN 0.8-cm FAT LAYER

		in front of abdomen: with a fat layer (0.8 cm thickness)					
Antenna Location (cm)	∞ (free space)	2.5	2.0	1.5	1.0	0.5	0.5
915 MHz dipole antenna half-length (cm) (radius = 0.127 cm)	7.7	7.7	7.7	7.7	7.7	7.7	7.0
input impedance (Ω)	75	53+j20	51+j18	52+j17	55+j20	66+j32	55-j1.2
input return loss (RL) to 50 Ω		14	15	15.6	14	10.5	26
input power P_i (W)	1	1	1	1	1	1	1
radiation power (to free space) P_{rad} (W)	1	0.492	0.405	0.312	0.218	0.135	0.123
body-absorbed power P_b (W)	0	0.520	0.600	0.690	0.779	0.857	0.858
sum of P_{rad} & P_b (W)	1	1.012	1.005	1.002	0.997	0.992	0.981
computation error (%)	0	1.2	0.5	0.2	0.3	0.8	1.9
peak-SAR (mW/g)	—	2.9	3.80	4.94	6.26	8.37	9.51
average-SAR (mW/g)	—	0.0087	0.010	0.010	0.013	0.014	0.0143

* The antenna input power is kept to be 1 W for comparison.

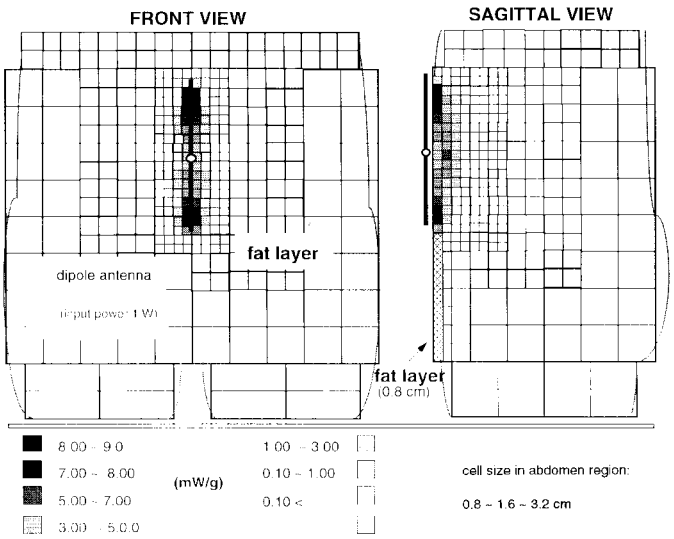

Fig. 4. 915-MHz SAR profile in the abdomen region (with an 0.8-cm fat layer) of a human body model. The dipole antenna applicator ($h = 7.7$ cm) is in front of the abdomen with a distance of 0.5 cm and the antenna input power is 1 W.

muscle phantom with a fat layer covering the abdomen. The electric parameters of the tissues at 915 MHz are [12]

- Muscle: $\epsilon = 51\epsilon_0$, $\sigma = 1.6$ S/m, mass density: $G = 1.04$ g/cm^3;
- Fat: $\epsilon = 5.6\epsilon_0$,. $\sigma = 0.1$ S/m, mass density: $G = 1.10$ g/cm^3.

Nonuniform cubic cells are used to model the whole body. The cell size ranges from 0.8 to 1.6 cm in the abdomen region around the antenna. Each cell is again partitioned into 27 subcells in the numerical integration of the associated matrix element. Approximately 54 000 subcells are involved in the computation. The thin-wire dipole antenna located adjacent to the abdomen is partitioned into 80 segments for numerical computation. With a radius 0.127 cm (0.1 in diameter), the approximate resonant half-length of a 915-MHz dipole antenna in free space is 7.7 cm. The free-space dipole input impedance is $75 + j1.3\ \Omega$, of which the reactance is approximately zero.

A. Without a Fat Layer

When the dipole antenna is located adjacent to the abdomen, due to the EM coupling effect, the input impedance of the dipole antenna now shifts away from resonance. Table I shows the input impedance and the return loss (relative to the 50-Ω system) of the free-space resonant dipole antenna at various

TABLE III
COMPUTATIONAL RESULTS OF THE SAR's, THE BODY-ABSORBED POWER, AND THE RADIATION POWER OF A 915-MHz DIPOLE ANTENNA APPLICATOR IN FRONT OF THE ABDOMEN OF A HUMAN BODY MODEL WITH A 1.6-cm FAT LAYER

		in front of abdomen: with a fat layer (1.6 cm thickness)					
Antenna Location (cm)	∞ (free space)	2.5	2.0	1.5	1.0	0.5	0.5
915 MHz dipole antenna half-length (cm)	7.7	7.7	7.7	7.7	7.7	7.7	6.7
(radius = 0.127 cm)							
input impedance (Ω)	75	61+j21	60+j21	60+j23	65+j27	73+j48	62-j4.8
input return loss (RL) to 50 Ω		14.6	14	13.8	11.6	7.9	18.7
input power P_i (W)	1	1	1	1	1	1	1
radiation power (to free space) P_{rad} (W)	1	0.477	0.403	0.326	0.245	0.203	0.191
body-absorbed power P_b (W)	0	0.528	0.598	0.672	0.746	0.783	0.803
sum of P_{rad} & P_b (W)	1	1.005	1.001	0.998	0.991	0.986	0.994
computation error (%)	—	0.5	0.1	0.2	0.9	1.4	0.6
peak-SAR (mW/g)	—	2.76	3.47	4.31	5.33	8.07	9.00
average-SAR (mW/g)	—	0.0088	0.010	0.011	0.012	0.013	0.0134

* The antenna input power is kept to be 1 W for comparison.

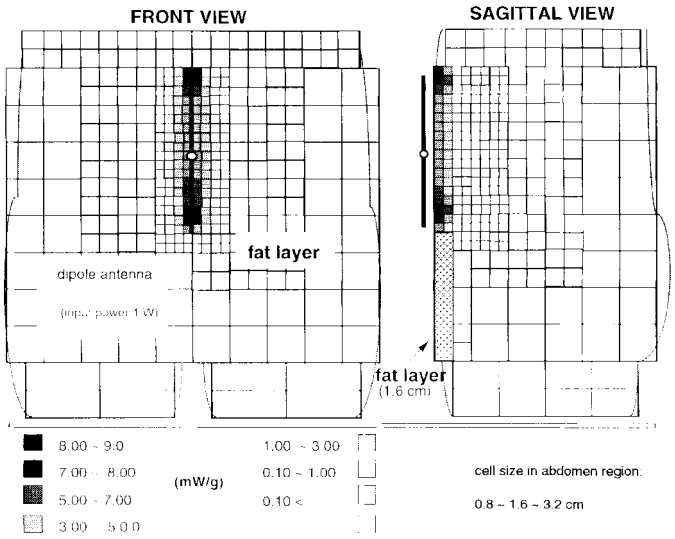

Fig. 5. 915-MHz SAR profile in the abdomen region (with a 1.6-cm fat layer) of a human body model. The dipole antenna applicator (h = 7.7 cm) is in front of the abdomen with a distance of 0.5 cm and the antenna input power is 1 W.

distances (0.5–2.5 cm) from the abdomen without a fat layer. The return loss can be used to determine the effective power input to the antenna applicator. Numerical results of the peak-SAR, average SAR, the power absorbed by the body, and EM radiation power to free space (from both the current of the antenna and the induced current in the body) are also shown in the table. Note that the antenna input power is kept to be 1 W for comparison. As expected, the EM power absorbed by the body and the SAR's (peak and average) increase with the shorter distance between the antenna and the body. When the distance is very close, for example, 0.5 cm, more than 90% of the EM power radiated from the antenna is absorbed by the body. For this case, the computed SAR distribution profiles of the abdomen part are plotted and shown in Fig. 3. It is observed that the hot spot is on the muscle surface and the SAR pattern is elliptical around the antenna feed point.

B. With a Fat Layer

1) Example 1—0.8-cm Fat Layer: Table II shows numerical results of the input impedance of the free-space-resonant dipole antenna at various distances (0.5–2.5 cm) from the abdomen, the peak SAR average SAR, the power absorbed by the body, and EM radiation power to free space (from both the antenna and the body). Again, it is observed that the body-absorbed power and the SAR's (peak and average) increase with the shorter antenna-body distance. Compared

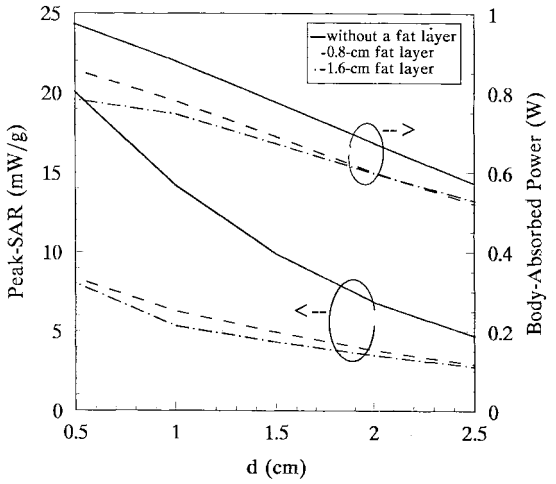

Fig. 6. Peak SAR and body absorbed power of various fat layer thickness versus the distance between the dipole antenna ($h = 7.7$ cm) and the abdomen at 915 MHz. The antenna input power is 1 W.

with the data listed in Table I (without a fat layer), it is observed that the peak SAR with a fat layer is much lower than those without a fat layer. This is because the fat tissue has much lower dielectric constant and conductivity than the muscle and hence will have less EM energy deposited into its tissue. For the 0.5-cm case, the computed SAR distribution profiles of the abdomen part are plotted and shown in Fig. 4. Two hot spots are observed on the fat surface near the ends of the antenna. This is consistent with the experimental measurements by Chou [1], [2]. The phenomenon of the greater energy deposition into fat, which is also reported by Chou [1], [2], is believed to be due to the proximity of the fat layer (overlaying the muscle) to the antenna, although the fat tissue is less conductive.

For the microwave hyperthermia heating purpose, the antenna applicator (adjacent to the abdomen) should be tuned to the near-resonant condition (approximate zero reactance) to enhance the EM energy deposited into the body. The resonant length of the dipole antenna and the input impedance for 0.5-cm distance from the abdomen are also shown in Table II, together with the associated peak SAR, average SAR, and the body-absorbed power. It can be observed that for the resonant antenna (adjacent to the abdomen), although the power absorbed by the body does not increase much, the peak SAR does increase about 15%.

2) Example 2—1.6-cm Fat Layer: Table III shows the input impedance and return loss of the free-space-resonant dipole antenna at various distances (0.5–2.5 cm) from the abdomen, the peak SAR, average SAR, the power absorbed by the body, and EM radiation power to free space (from both the antenna and the body). For the 0.5-cm case, the computed SAR distribution profiles of the abdomen part are plotted and shown in Fig. 5. Again, two hot spots are observed on the fat surface near the ends of the antenna. The sagittal SAR pattern shows very low EM energy penetration in muscle for this 1.6-cm fat layer case. A thick fat layer will behave like a "shield" to cause less EM-energy penetration into the muscle tissue. Table III also lists results of the tuned antenna (to resonant condition) for the 0.5-cm distance. The peak SAR increases about 12%.

The consistancy of the numerical computation can be monitored by checking the sum of the body-absorbed power and the radiation power to free space, which should be equal to the antenna input power. As shown in Tables I–III, the computation error is lower than 2%. Fig. 6 depicts the variation of the peak SAR and the body-absorbed power of various fat layer thickness versus the distance between the dipole antenna and the abdomen at 915 MHz (1-W antenna input power). As observed, the SAR and the body absorbed power decrease with distance and the peak SAR is about 50% lower for the fat layer case.

IV. Conclusion

The effects of the fat layer on the microwave near-field radiation to the abdomen of a full-scale human body model have been studied. The human body is modeled as a homogeneous muscle phantom with a fat layer covering the abdomen. The dipole wire-antenna is used to simulate the microwave hyperthermia RF applicator or the wireless communication handset antenna. CIE and the MoM are employed to numerically compute the penetrating EM energy from the radiating antenna into the proximate abdomen. Nonuniform cells and a 27 subcells' scheme are used to model the whole body for efficient numerical computation. EM energy deposition into the body (especially the abdomen) with and without a fat layer at 915 MHz are presented and compared. While a hot spot is observed on the muscle surface near the antenna feed point location for the pure muscle body, two hot spots on the fat surface near the ends of the antenna are observed. This is consistent with the reported experimental measurements. It is found that the peak SAR, average SAR, and total power absorbed by the body with a fat layer are much lower than those without a fat layer. The peak SAR is about 50% lower. For 1.6-cm fat layer, the sagittal SAR pattern shows very low EM energy penetration in muscle and most of the heating is in the fat layer. A thick fat layer will shield the muscle tissue and causes less EM energy penetration from the RF antenna applicator into the muscle tissue. The tuned resonant-antenna can increase the peak-SAR about 10%–15%. These effects are important for the microwave hyperthermia heating and near-field RF hazard assessment of the wireless communication handset antenna.

References

[1] C. K. Chou, J. A. McDougall, K. W. Chan, and K. H. Luk, "Effects of fat thickness on heating patterns of the microwave applicator," *Int. J. Radiation Oncology Biol. Phys.*, vol. 19, no. 4, pp. 1067–1070, Oct. 1990.

[2] C. K. Chou, "Evaluation of microwave hyperthermia applicators," *Bioelectromagnetics*, vol. 13, pp. 581–597, 1992.

[3] K. S. Yee, "Numerical solution of initial boundary value problem involving Maxwell's equations in isotropic media," *IEEE Trans. Antennas Propagat.*, vol. AP-14, pp. 302–307, May 1966.

[4] A. Taflove and M. E. Brodwin, "Numerical solution of steady-state electromagnetic scattering problems using the time-dependent Maxwell's equations," *IEEE Trans. Microwave Theory Tech.*, vol. MTT-23, pp. 623–630, Aug. 1975.

[5] J. Toftgard, S. N. Hornsleth, and J. B. Andersen, "Effects on portable antennas of the presence of a person," *IEEE Trans. Antennas Propagat.*, vol. 41, pp. 739–746, June 1993.
[6] P. J. Dimbylow, "FDTD calculation of the SAR for a dipole closely coupled to the head at 900 MHz and 1.9 GHz," *Phys. Med. Biol.*, vol. 38, pp. 361–368, Feb. 1993.
[7] M. A. Jensen and Y. R.-Samii, "EM Interaction of handset antennas and a human in personal communications," *Proc. IEEE*, vol. 83, no. 1, pp. 1–17, Jan. 1995.
[8] D. Sullivan, "Three-dimensional computer simulation in deep regional hyperthermia using the finite-difference time-domain method," *IEEE Trans. Microwave Theory Tech.*, vol. 38, no. 2, pp. 204–211, Feb. 1990.
[9] H.-R. Chuang, "Human operator coupling effects on radiation characteristics of a portable communication dipole antenna," *IEEE Trans. Antennas Propagat.*, vol. 42, pp. 556–560, Apr. 1994.
[10] K. Karimullah, K.-M. Chen, and D. P. Nyquist, "Electromagnetic coupling between a thin-wire antenna and a neighboring biological body: Theory and experiment," *IEEE Trans. Microwave Theory Tech.*, vol. MTT-28, no. 11, pp. 1218–1225, Nov. 1980.
[11] S. Silver, *Microwave Antenna Theory and Design*. Piscataway, NJ: IEEE Press, 1986, pp. 80–88.
[12] C. C. Johnson and A. W. Guy, "Nonionizing electromagnetic wave effects in biological materials and systems," *Proc. IEEE*, vol. 60, pp. 692–718, June 1972.

H.-R. Chuang was born in Tainan, Taiwan, R.O.C., on August 18, 1955. He received the B.S.E.E. and M.S.E.E. degrees from the National Taiwan University, Tainan, Taiwan, in 1977 and 1980, respectively, and Ph.D. degree in electrical engineering from Michigan State University, East Lansing, in 1987.

From 1987 to 1988, he was a Post Doctoral Research Associate at the Engineering Research Center, Michigan State University. From 1988 to 1990, he was with the Portable Communication Division, Motorola Inc., Ft. Lauderdale, FL. Since 1991, he has been with the Department of Electrical Engineering, National Cheng Kung University, Tainan, Taiwan, as an Associate Professor. His research interests include numerical computation of the EM interaction between antennas and the human body, portable antennas design for wireless communications, computational electromagnetics for EMI/EMC problems, satellite reflector antennas, RF/microwave communication circuits design, and microwave detection systems.

Dr. Chuang received the Distinguished Paper Award (EM section) of the 1994 National Symposium on Communications, Taiwan R.O.C., for the research of the satellite-shaped reflector antenna design for contoured beam synthesis.